Cement and Concrete Research 39 (2009) 957–965

Contents lists available at ScienceDirect

Cement and Concrete Research

journal homepage: http://ees.elsevier.com/CEMCON/default.asp

# Determining the water–cement ratio, cement content, water content and degree of hydration of hardened cement paste: Method development and validation on paste samples

H.S. Wong [*], N.R. Buenfeld

*Concrete Durability Group, Imperial College London, SW7 2AZ, UK*

ARTICLE INFO

*Article history:*
Received 1 July 2007
Accepted 12 June 2009

*Keywords:*
Backscattered electron imaging (B)
Image analysis (B)
Microstructure (B)
SEM (B)
*w/c* ratio

ABSTRACT

We propose a new method to estimate the initial cement content, water content and free water/cement ratio (*w/c*) of hardened cement-based materials made with Portland cements that have unknown mixture proportions and degree of hydration. This method first quantifies the composition of the hardened cement paste, i.e. the volumetric fractions of capillary pores, hydration products and unreacted cement, using high-resolution field emission scanning electron microscopy (FE-SEM) in the backscattered electron (BSE) mode and image analysis. From the obtained data and the volumetric increase of solids during cement hydration, we compute the initial free water content and cement content, hence the free *w/c* ratio. The same method can also be used to calculate the degree of hydration. The proposed method has the advantage that it is quantitative and does not require comparison with calibration graphs or reference samples made with the same materials and cured to the same degree of hydration as the tested sample. This paper reports the development, assumptions and limitations of the proposed method, and preliminary results from Portland cement pastes with a range of *w/c* ratios (0.25–0.50) and curing ages (3–90 days). We also discuss the extension of the technique to mortars and concretes, and samples made with blended cements.

## 1. Introduction

The mass ratio of water-to-cement content is one of the most fundamental parameters in concrete mixture proportioning. The *w/c* ratio has a significant influence on most properties of hardened concrete in particular strength and durability [1] due to its relationship with the amount of residual space i.e. capillary porosity, in the cement paste. Since the *w/c* ratio is an indication of the quality of a concrete mix, the situation often arises where it is desirable to examine the original *w/c* ratio of a particular concrete some time after it has hardened. This is often carried out in disputes when non-compliance with the mix specification is suspected. Determination of the *w/c* ratio is also important for quality control during concrete production and general quality assurance purposes.

Unfortunately, once concrete has set, it is very difficult to ascertain the exact amounts of cement and water that were originally added during batching. There is yet to be a standardised and universally accepted technique for accurately determining the original *w/c* ratio of a sample taken from an existing structure [2]. BS 1881: part 124: 1988 [3] describes a physico-chemical method to calculate the original *w/c* ratio by separate estimations of the original cement content from partial chemical analysis (for soluble silica and calcium oxide) and original water content from the sum of chemically bound water and the volume of capillary pores, which in turn, is obtained from vacuum saturation of a dried sample with a liquid of known density. This method cannot be used for concretes that are damaged, either physically or chemically, concretes that are poorly compacted and concretes with entrained air or unusually porous aggregates. This method is also known to have a low precision, estimated to be within 0.1 (*w/c* ratio, by mass) [4] or even greater [2,5], and therefore has little practical value.

Nordtest Build NT 361-1999 [6] describes a method for estimating *w/c* ratio using fluorescence microscopy. The sample is first impregnated with a resin containing fluorescent dye. A polished thin-section of the sample is then produced and subsequently examined using a petrographic microscope. The intensity of the fluorescence emitted from the cement paste is proportional to the amount of intruded resin, which in turn is related to the capillary porosity and the *w/c* ratio. Indeed, many studies have confirmed that the change in fluorescence intensity could be related to a change in *w/c* ratio [5,7–10]. Hence, if a set of suitable reference standards made of a similar concrete with known *w/c* ratio is available, one can allocate an equivalent *w/c* ratio to the sample in question by visual comparison. Sahu et al. [11] proposed another microscopy-based method to estimate the *w/c* ratio of hardened concrete. Using scanning electron microscopy in the backscattered electron (BSE) mode, the authors measured the

---

[*] Corresponding author. Tel.: +44 20 7594 5957; fax: +44 20 7225 2716.
*E-mail address:* hong.wong@imperial.ac.uk (H.S. Wong).

0008-8846/$ – see front matter © 2009 Elsevier Ltd. All rights reserved.
doi:10.1016/j.cemconres.2009.06.013

capillary porosity thresholded at grey level <50 at standardised brightness and contrast settings. This was plotted against *w*/*c* ratio for a set of reference samples and a good linear correlation was obtained. The equation of the best-fit line was subsequently used to calculate the *w*/*c* ratio of unknown samples.

The main drawback of the current microscopy-based methods is the need to use reference standards for comparison or calibration purposes. In the fluorescence microscopy method, the reference standards need to have the same cement and aggregate type, air void content and degree of hydration, in addition to the *w*/*c* ratio, as the concrete being examined [2,5]. In the electron microscopy method, the reference standards should have the same degree of hydration as the tested sample. For field concretes, the materials used may not be known or available. If the materials are known and available, the curing and exposure history is usually unknown. The curing and exposure history affect the degree of hydration, which influences the capillary porosity and the amount of intruded resin. Therefore, it has been recommended that these techniques be only used for relatively mature Portland cement concrete, but whether this precautionary measure is sufficient or not is debatable.

In this paper, we propose a new microscopy-based method for estimating the *w*/*c* ratio that does not require comparison to any reference standards. We are interested in the 'free' *w*/*c* ratio, i.e. the amount of water present in the mix at the time of setting excluding any water 'lost' to aggregate absorption and evaporation. The free *w*/*c* ratio is more relevant than the total *w*/*c* ratio for ascertaining concrete quality because the absorbed and evaporated water prior to setting plays no part in the formation of capillary pores. The method is also able to determine the initial free water and cement content, and the degree of hydration of an unknown mix composition. This paper reports the development, assumptions and limitations of the proposed method, and preliminary results from Portland cement pastes with a range of *w*/*c* ratios and curing ages. Pastes were chosen for this preliminary study since they can be prepared with well-controlled free *w*/*c* ratio. We also discuss the extension of the technique to mortars and concretes, and samples made with blended cements.

## 2. Proposed method

### 2.1. Theoretical development

The chemistry of Portland cement hydration is complex and not fully understood, although much progress has been made over the years. In the simplest representation, cement reacts with water to form products of hydration, which precipitate out from a saturated solution to form solids. The hydration products consist of crystalline (CH, AFt, AFm) among others and non-crystalline (C–S–H gel) phases having different physical and chemical properties, but for simplicity, they will be considered collectively as a single component in this paper. The solid hydration products occupy a greater volume than the volume of the reacted cement, but slightly smaller than the sum of the volumes of the cement and water due to chemical shrinkage. As a result of the increase in the total solids volume, the originally water-filled spaces (capillary pores) become progressively filled with time.

At any moment after setting, the hardened cement paste can be thought to consist of four main components: a) the remaining unreacted cement; b) the crystalline and semi-crystalline hydration products, including their intrinsic 'gel pores'; c) the capillary pores and d) air voids from incomplete compaction and deliberate entrainment. This is schematically represented in Fig. 1. The sum of the absolute volumes of these four components and any shrinkage must be equal to the total volumes of the original cement content, free water and air voids at the time of set. The total shrinkage is small and negligible for the purpose of this investigation (see Discussion). We assume that the volume of entrapped and entrained air is invariant with time since the hydration products are expected to occupy the water-filled capillary pores only. Therefore, at any hydration degree, we can write:

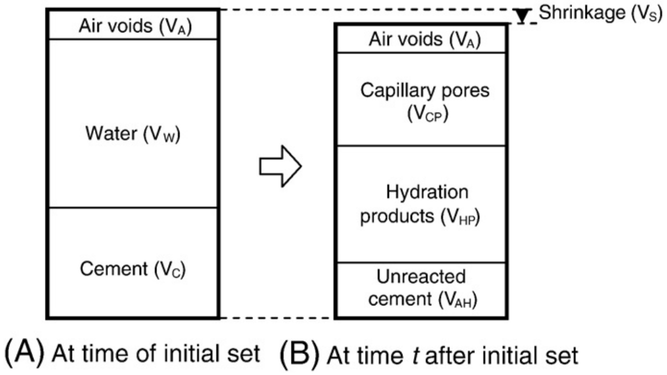

**Fig. 1.** Schematic representation of the volumetric proportions of the main components in hardened cement paste at time of initial set (A) and at time *t* after setting (B).

$$V_C + V_W = V_{AH} + V_{HP} + V_{CP} \tag{1}$$

where $V_C$, $V_W$, $V_{AH}$, $V_{HP}$ and $V_{CP}$ represent absolute volumes of the original cement, original free water, unreacted (anhydrous) cement, hydration products and capillary pores. Next, we consider the volumetric ratio of hydration products to the reacted cement, which we call $\delta_V$ in this paper. It is well known that for any room temperature cured contemporary Portland cements at any *w*/*c* ratio and age, the cement hydration products occupy approximately twice the volume of reacted cement, i.e. $\delta_V \sim 2$. The actual value of $\delta_V$ is slightly dependent on the cement composition (shown later), and typical values of between 2.1 and 2.2 have been reported in the literature [1,12,13]. Thus:

$$V_C = V_{AH} + \frac{V_{HP}}{\delta_V} \tag{2}$$

and from (1):

$$V_W = V_{AH} + V_{HP} + V_{CP} - \left(V_{AH} + \frac{V_{HP}}{\delta_V}\right) = V_{HP}\left(1 - \frac{1}{\delta_V}\right) + V_{CP} \tag{3}$$

Therefore, if the specific gravity of cement is $\rho_c$, we can express the free *w*/*c* ratio as:

$$\frac{w}{c} = \frac{V_W}{V_C \times \rho_c} = \frac{V_{HP}(\delta_V - 1) + \delta_V V_{CP}}{(\delta_V V_{AH} + V_{HP})\rho_c} \tag{4}$$

The degree of hydration ($m$) can be estimated from the fraction of cement reacted. By substituting $V_c$ with Eq. (2), we can express the degree of hydration as:

$$m = \frac{V_C - V_{AH}}{V_C} = \frac{V_{HP}}{\delta_V V_{AH} + V_{HP}} \tag{5}$$

Thus, it appears that the original cement content, free water content, free *w*/*c* ratio and the degree of hydration can be determined, at any time after setting, from the volumetric ratio of hydration products to the reacted cement $\delta_V$ and the volumetric fractions of the unreacted cement, hydration products and capillary pores at the time of test. The latter may be directly measured using microscopy and image analysis techniques. The application of the method does not require prior knowledge of the original cement content and is not affected by curing age; hence it may be suitable for testing field samples. However, the method will require: 1) a precise description of $\delta_V$, 2) the ability to image the capillary pores, hydration products and unreacted cement, and 3) an accurate and reproducible image analysis routine to segment and quantify these.

### 2.2. Derivation of $\delta_V$ from Powers and Brownyard's model

As stated earlier, a good first approximation for $\delta_V$ is 2 since Portland cements form hydration products that occupy about twice the volume of reacted cement at any *w*/*c* ratio and age. The actual value of $\delta_V$, however, is slightly dependent on the cement composition and this can be derived from the work of Powers and Brownyard [14]. Powers and Brownyard [14] proposed that water in cement paste can be classified as evaporable (capillary and gel water) and non-evaporable (chemically bound water). The gel water is the water adsorbed by the fine nanoscale characteristic pores in the hydration products. Accordingly, the volume of the hydration products ($V_{HP}$) and reacted cement ($V_{C'}$) can be written as:

$$V_{HP} = c'v_c + w_n v_n + w_g v_g \quad \text{and} \quad V_{C'} = mcv_c \tag{6}$$

where $c'$, $w_n$ and $w_g$ are the mass of the reacted cement, non-evaporable water and gel water respectively, and $\upsilon_c$, $\upsilon_n$ and $\upsilon_g$ are the specific volumes of the cement, non-evaporable water and gel water respectively. The volumetric ratio of hydration products to the reacted cement $\delta_V$ is thus:

$$\delta_V = \frac{V_{HP}}{V_{C'}} = \frac{c'v_c + w_n v_n + w_g v_g}{mcv_c} = 1 + \frac{w_n}{c'}\frac{v_n}{v_c} + \frac{w_g}{c'}\frac{v_g}{v_c} \tag{7}$$

To apply Eq. (7), the functions $w_n/c'$ and $w_g/c'$, which are the non-evaporable water per mass of hydrated cement and the gel water per mass of hydrated cement respectively, and the specific volumes of the non-evaporable water and gel water, need to be known. Powers and Brownyard [14] performed numerous experiments on neat cement pastes and mortars made with 86 types of cement (commercial and laboratory prepared) of different compositions at various *w*/*c* ratios (0.31–0.61) and curing ages (7–479 days) and found that these functions are relatively constant, and only slightly dependent on the cement composition. This is a crucial finding because it suggests that all Portland cements hydrate at room temperature to form approximately the same hydration products, at approximately the same rate and mutual proportions [15,16].

Powers and Brownyard [14] determined the non-evaporable water content ($w_n$) by ignition to 1000 °C following P-drying (in an evacuated desiccator over $Mg(ClO_4).2H_2O$ until constant mass), which removed the evaporable water first. They observed that $w_n$ mainly depended on the amount of reacted cement and the ratio $w_n/c'$ can be approximated as a function of the clinker mineral composition:

$$\frac{w_n}{c'} = 0.187x_{C_3S} + 0.158x_{C_2S} + 0.665x_{C_3A} + 0.213x_{C_4AF} \tag{8}$$

where $x$ represent the mass fractions of the $C_3S$ (alite), $C_2S$ (belite), $C_3A$ (aluminate) and ferrite ($C_4AF$). To obtain the gel water content, Powers and Brownyard [14] then performed water vapour sorption experiments on the P-dried samples and found that the amount of water held at RH below 45% is proportional to the amount of cement reacted, and thus to the gel pore volume, and that at RH greater than 45%, the water condenses in the larger capillary pores. Applying B.E.T. theory to the measured adsorption isotherm, Powers and Brownyard [14] then introduced and measured the property $V_m/w_n$, where $V_m$ corresponds to the mass of water to cover the hydration products with a single monolayer of water, this being achieved at RH of about 20%. Thus, the ratio $V_m/w_n$ represents the specific internal surface and again, they found that this is relatively constant with *w*/*c* ratio and curing age, but depends on the cement composition. The following empirical fit was obtained:

$$\frac{V_m}{w_n} = 0.230x_{C_3S} + 0.320x_{C_2S} + 0.317x_{C_3A} + 0.368x_{C_4AF} \tag{9}$$

Powers and Brownyard [14] further observed that the maximum amount of water that can be retained by the hydration product, i.e. gel water, corresponds to $4V_m$. Therefore, the parameter $w_g/c'$ in Eq. (7) can be obtained by multiplying the experimentally derived $w_n/c'$ (Eq. (8)) and $4V_m/w_n$ (Eq. (9)). The non-evaporable water and gel water were considered to be 'compressed' i.e. having specific volumes ($v_n$ and $v_g$ respectively) lower than that of the free water ($=1$ cm$^3$/g). Using a pycnometer and helium displacement measurements on P-dried samples, it was found that the specific volume of non-evaporable water ($v_n$) did not vary much for all examined pastes and that the value of 0.72 cm$^3$/g was representative [16]. Subsequently, the specific volume of gel water ($v_g$) could be determined indirectly as 0.90 cm$^3$/g.

Powers and Brownyard's [14] classification of water in cement paste is somewhat arbitrary since an overlap in binding energies of the water phases is expected, but their model allows quantitative calculation of the cement paste composition and explains many different properties of the cement paste [15,17]. Although the accuracy with which the non-evaporable water and gel water can be separately measured is questionable, the sum of the non-evaporable and gel water content is useful and remains relevant to this study. Some of the gel water or even the non-evaporable water is probably removed during drying when measuring capillary porosity. However, a similar condition occurs in samples prepared for electron microscopy, and thus the value $\delta_V$ is transferable to this technique.

## 3. Experimental

### 3.1. Materials and sample preparation

Five ordinary Portland cement pastes with *w*/*c* ratios 0.25, 0.30, 0.35, 0.40 and 0.50 were prepared using cement complying with BSEN197-1-CEM 1 and tap water. The cement has a Blaine specific surface area and specific gravity of 342 m$^2$/kg and 3.15 respectively. Its mineral composition, calculated from the modified form of the Bogue calculation [19], is 63% alite, 12.8% belite, 7.4% aluminate and 8.3% ferrite. Therefore, using Eqs. (7)–(9), its $\delta_V$ is 2.02.

The mixing was done using a bowl mixer and the samples were compacted in two equal layers into plastic cylindrical moulds (58 mm diameter, 49 mm height) using a vibrating table with adjustable intensity. For each layer, compaction was assumed complete when no significant amount of air bubbles escaped the surface. The samples were then capped and sealed, taking care to minimise any entrapped air. Subsequently, they were rotated slowly for 24 h to avoid bleeding and segregation effects.

After the initial 24 h, the samples still in their plastic containers, were wrapped in cling film and sealed in polythene bags at 20 °C until the ages of 3, 7, 28 and 90 days. At the end of each curing age, one cylinder was sectioned at mid-height using a diamond saw to produce a rectangular block sample (40×20×8 mm) for microscopy. The block samples were freeze-dried to remove the pore water and then impregnated with low viscosity epoxy (pre-heated to 50 °C and thinned with toluene) using the methodology described by Wong and Buenfeld [20]. It is critical to ensure that the blocks are properly impregnated with epoxy to preserve the delicate microstructure and to provide atomic contrast to the capillary pores. The epoxy impregnated blocks were cured for several days at room temperature to allow proper hardening of the epoxy. Following this, they were ground and polished with diamond in the usual manner at successively finer grades to a 1/4-μm finish.

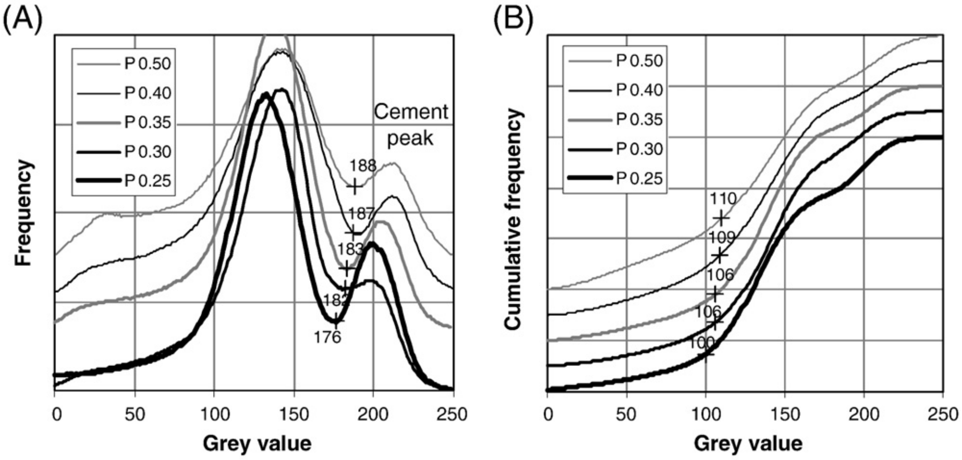

**Fig. 2.** Segmentation of the unreacted cement and capillary pores. The threshold (marked as +) for unreacted cement is selected from the minimum between peaks for hydration products and unreacted cement on the brightness histogram (A). The threshold for porosity is obtained from the inflection point of the cumulative brightness histogram (B).

### 3.2. BSE imaging

The volume fractions of unreacted cement, hydration products and capillary pores were measured by image analysis on backscattered electron (BSE) images [17]. A Camscan Apollo 300 FE-SEM was used for BSE imaging. The FE-SEM gives a better resolving power than conventional SEM because the brighter and more stable electron source is able to produce a higher density beam, but at smaller beam size and at lower energy [18]. Prior to imaging, the brightness and contrast settings of the microscope were calibrated so that the brightness histogram of the recorded image was centred and stretched to span the entire dynamic range of the available grey scale (0 to 255) for each image. This required a trial and error approach, but once the optimum brightness and contrast setting had been found, the same setting was applied to all subsequent images. This is important to ensure a faithful reproduction of grey values in every image over the entire range of samples investigated so that a meaningful comparison and accurate quantitative data can be obtained.

Imaging was performed at low vacuum (40 Pa), so no sample coating was necessary to avoid charging effects. Thirty images were collected randomly for each sample by programming the stage to move in a grid fashion and stopping at predefined, equally spaced co-ordinates, spanning the entire sample surface. This provided a systematic sampling approach to ensure that sampling was random

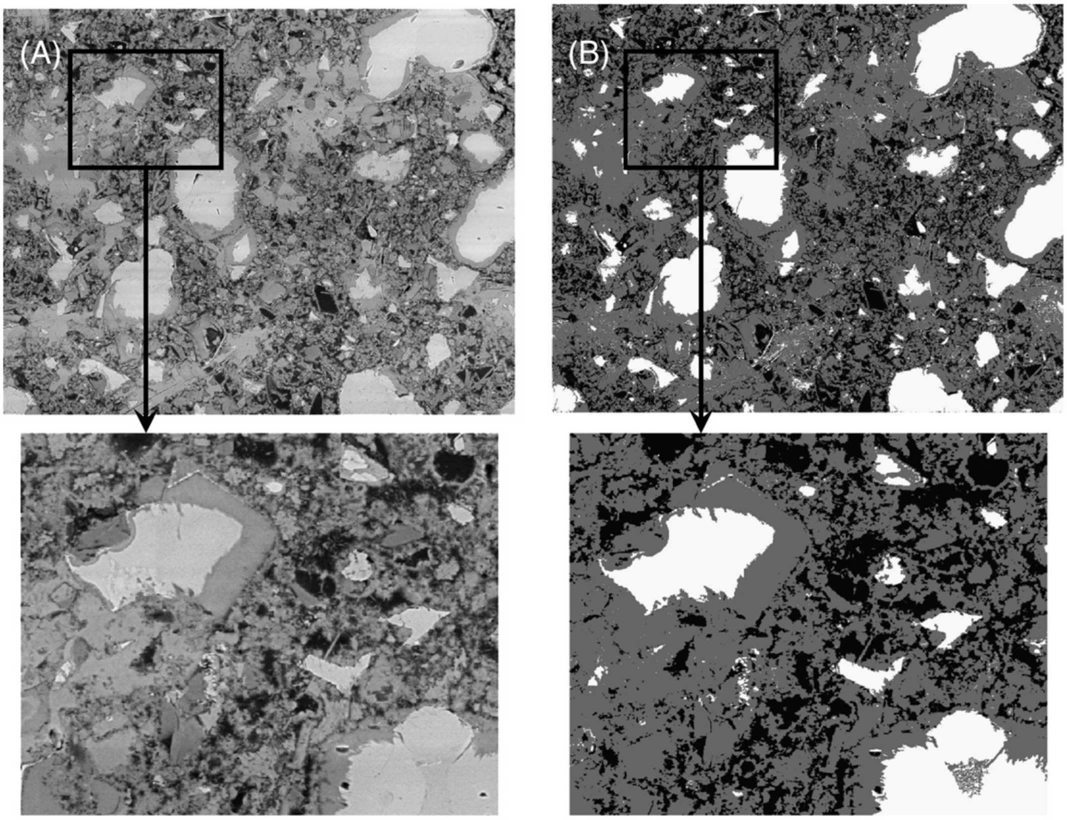

**Fig. 3.** Comparison between an original BSE image (A) and the segmented image (B) for measuring the volume fractions of the unreacted cement (white pixels), hydration products (dark grey pixels) and capillary pores (black pixels). Insets show magnified portions of the original images, highlighting the effectiveness of the segmentation procedure. The sample is a *w*/*c* 0.4 paste cured for 3 days. Field of view is 240 × 192 µm (67 × 54 µm for insets).

and uniform. The images were captured at 10 kV accelerating voltage, 10 mm working distance and 500x magnification. The images were digitised to 2560 × 2048 pixels at a pixel spacing of 0.094 µm, giving an image field of view of 240 × 192 µm. This magnification and pixel spacing level was chosen as a compromise to obtain adequate resolution and a representative sampling area.

### 3.3. Image analysis

The unreacted cement, hydration products and capillary pores are segmented from the BSE images to allow measurement of their area and volumetric fractions using stereology [21]. Segmentation is the first step in quantitative image analysis and also the most crucial because all subsequent measurements are carried out on the segmented image. An appropriate thresholding method must be employed so that the results are accurate and reproducible. However, segmentation of a digital image can never be error free due to various reasons such as the finite-pixel size effect and the overlapping of signal sampling volumes. Nevertheless, these errors can be reduced by using an objective and consistent thresholding rule.

The unreacted cement particles are highly contrasted from the hydration products so segmentation is relatively easy by selecting the minimum grey value between peaks for hydration products and the unreacted cement as the lower threshold value (Fig. 2A). The exact location of the minima is determined from the first derivative of the brightness histogram. The capillary pores are segmented using the 'overflow' method proposed by Wong et al. [22], whereby the inflection point of the cumulative brightness histogram is taken as the upper threshold value. This is obtained from the intersection of two best-fit lines in the cumulative brightness histogram. For the purpose of this study, the capillary porosity is considered to include the hollow shell pores since Powers and Brownyard's model does not distinguish the latter pore type. Microcracks due to damage caused by the sample preparation should not be included and care was taken to avoid imaging these areas, in particular near the sample edges. Nevertheless, the amount of microcracking observed in the samples was small and therefore considered not to have a significant influence.

Fig. 2A and B show examples of the obtained thresholds for unreacted cement and capillary pores, selected from the range of samples investigated. Note that the histograms are vertically offset to improve clarity. The absolute threshold values are not constant, but vary slightly due to small (and unavoidable) fluctuations of the beam conditions, chamber pressure or specimen surface conditions. Nevertheless, since every image is thresholded using consistent rules, the effect of this on the measured volumetric fraction is small. Finally, the volume fraction of hydration products is obtained by simple subtraction, taking care to exclude any entrapped air voids, which can be easily distinguished due to their large size and spherical shape.

Fig. 3 shows an example of the original BSE image and the segmented image, highlighting the effectiveness of the segmentation procedure. The volume fractions obtained from each frame are then used to calculate the 'local' cement content, free water content, free *w*/*c* ratio and degree of hydration, using Eqs. (2)–(5). This is repeated for a large number of frames (typically 30 images are required) until their cumulative averages from successive frames do not vary significantly, thereby indicating that a representative volume has been analysed.

### 3.4. Degree of hydration

The degree of hydration was estimated using the proposed method (Eq. (5)) and the results compared to the conventional method of measuring the non-evaporable water content by loss-on-ignition (LOI). At the end of each curing age, the remaining pieces (~35 g) from each cylindrical sample were dried in an oven at 105 °C until constant mass to remove all evaporable water, then crushed and heated to

**Table 1**
Measured volume fractions of unreacted cement, hydration products and capillary porosity from image analysis (average of 30 frames at each age), estimated *w*/*c* and the degree of hydration from loss-on-ignition.

| Sample | Unreacted cement (%) | | | | Hydration products (%) | | | | Porosity (%) | | | | Estimated *w*/*c* | | | | Hydration degree *m*(LOI) | | | |
|---|---|---|---|---|---|---|---|---|---|---|---|---|---|---|---|---|---|---|---|---|
| | 3d | 7d | 28d | 90d | 3d | 7d | 28d | 90d | 3d | 7d | 28d | 90d | 3d | 7d | 28d | 90d | 3d | 7d | 28d | 90d |
| P 0.50 | 14.8 (0.5) | 11.0 (0.5) | 7.8 (0.4) | 6.1 (0.4) | 47.9 (0.6) | 58.6 (0.6) | 64.7 (0.6) | 65.2 (0.5) | 37.3 (0.4) | 30.4 (0.5) | 27.5 (0.4) | 28.6 (0.4) | 0.51 (0.007) | 0.48 (0.007) | 0.48 (0.004) | 0.51 (0.005) | 0.69 | 0.70 | 0.77 | 0.88 |
| P 0.40 | 15.8 (0.8) | 14.4 (0.5) | 10.5 (0.5) | 10.1 (0.5) | 55.9 (0.7) | 62.8 (0.6) | 70.2 (0.6) | 68.2 (0.9) | 28.4 (0.6) | 22.8 (0.4) | 19.3 (0.3) | 21.6 (0.7) | 0.42 (0.009) | 0.38 (0.004) | 0.38 (0.004) | 0.41 (0.007) | 0.64 | 0.67 | 0.72 | 0.87 |
| P 0.35 | 17.4 (0.5) | 18.11 (0.8) | 14.6 (0.7) | 13.3 (0.6) | 59.4 (0.4) | 61.4 (0.9) | 67.3 (0.6) | 69.7 (0.7) | 23.3 (0.4) | 20.5 (0.5) | 18.1 (0.3) | 17.0 (0.3) | 0.36 (0.005) | 0.34 (0.005) | 0.35 (0.005) | 0.35 (0.004) | 0.59 | 0.61 | 0.73 | 0.80 |
| P 0.30 | 23.5 (0.7) | 21.6 (0.6) | 17.2 (0.5) | 16.2 (0.6) | 56.2 (0.6) | 58.9 (0.7) | 67.8 (0.5) | 68.6 (0.7) | 20.3 (0.4) | 19.5 (0.5) | 14.9 (0.3) | 15.1 (0.2) | 0.30 (0.005) | 0.31 (0.005) | 0.31 (0.004) | 0.32 (0.004) | 0.54 | 0.58 | 0.66 | 0.69 |
| P 0.25 | 27.9 (0.7) | 27.8 (0.9) | 25.2 (0.8) | 22.6 (0.7) | 57.5 (0.7) | 58.5 (0.8) | 62.2 (0.6) | 64.4 (0.8) | 14.6 (0.3) | 13.8 (0.3) | 12.6 (0.3) | 13.0 (0.3) | 0.25 (0.004) | 0.24 (0.005) | 0.25 (0.005) | 0.27 (0.004) | 0.48 | 0.49 | 0.57 | 0.62 |

Values in parentheses represent the respective standard errors.

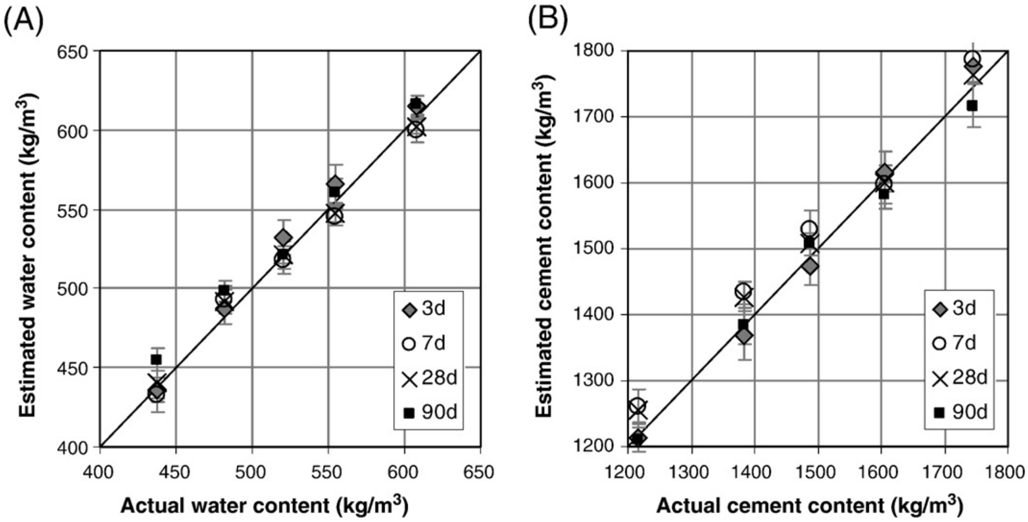

**Fig. 4.** Comparison between the estimated and actual values of the original water content (A) and cement content (B) for all samples investigated. The error bars represent 95% confidence interval.

1050 °C for 3 h. The non-evaporable water was taken as the mass loss between 105 °C and 1050 °C, corrected for the LOI of the dry cement powder (=1.36%). The degree of hydration, $m$(LOI), was then calculated as the ratio of the non-evaporable water content per gram cement to the amount at complete hydration, which is assumed to be equal to 0.23 g/g for OPC.

The degree of hydration was also estimated by using a conventional image analysis method that first measures the volume fraction of the unreacted cement ($V_{\mathrm{AH}}$) from BSE images. If the original cement content of the sample ($V_{\mathrm{C}}$) is known a priori, then the degree of hydration, $m$(IA), can be calculated as:

$$m(\mathrm{IA}) = 1 - \frac{V_{\mathrm{AH}}}{V_{\mathrm{C}}} \quad (10)$$

Note that our proposed method (Eq. (5)), in contrast to the conventional image analysis method (Eq. (10)), does not require prior knowledge of the original cement content.

## 4. Results

The average volume fractions of unreacted cement, hydration products and capillary porosity measured from image analysis and the average degree of hydration measured from the non-evaporable water content for all samples are given in Table 1. As expected, samples with lower *w*/*c* ratios have higher unreacted cement content and lower capillary porosity. The degree of hydration from LOI for all *w*/*c* ratios and curing ages ranged between 0.48 and 0.88. For samples at the same *w*/*c* ratio, the unreacted cement content and detectable capillary porosity decreases with an increase in hydration degree.

Taking $\delta_{\mathrm{V}}$ equal to 2.02 and the specific gravity of cement as 3.15, the original cement content, water content and free *w*/*c* ratio are calculated using Eqs. (2)–(4). The results are plotted against their actual values in Figs. 4 and 5. The *y*-axis error bars for each data point indicate the 95% confidence interval calculated using Student's *t*-distribution.

The local variation in *w*/*c* ratio is indicated more clearly in the frequency distribution histograms shown in Fig. 6. For instance, for the paste samples cast with original *w*/*c* ratio of 0.35, the estimated *w*/*c* ratio at each image location (representing an area of 240×192 µm) for all 120 images was found to range from 0.25 to 0.45. This apparently large range in the local *w*/*c* ratio is not surprising because cement-based materials are known to be heterogeneous at the micro-scale. The observed variability also depends on the field of view, and is expected to increase with smaller imaged area, which is a trade-off for better resolution. Nevertheless, when a representative number of frames are measured and averaged, there appears to be a generally good agreement between the estimated and the actual values for the water content, cement content and *w*/*c* ratio across all samples and curing ages investigated (Figs. 4 and 5). As mentioned in section 3.3, the number of images required for a representative measurement can be determined from a plot of cumulative averages with successive frames analysed.

In Fig. 7, the estimated degree of hydration is compared against the measured values from the LOI test (Fig. 7a) and conventional image analysis (Fig. 7b). Again, a relatively good agreement between the estimated and measured values is observed for both cases. It is interesting to note that the correlation with the conventional image analysis method is slightly better when compared to the LOI method. This suggests that some errors may stem from the LOI test such as 1) dehydration of the C–S–H, AFm and Aft phases may have occurred at temperatures below 105 °C, making the LOI results lower than actual values, and 2) the mass loss between 105 °C and 1050 °C may also be

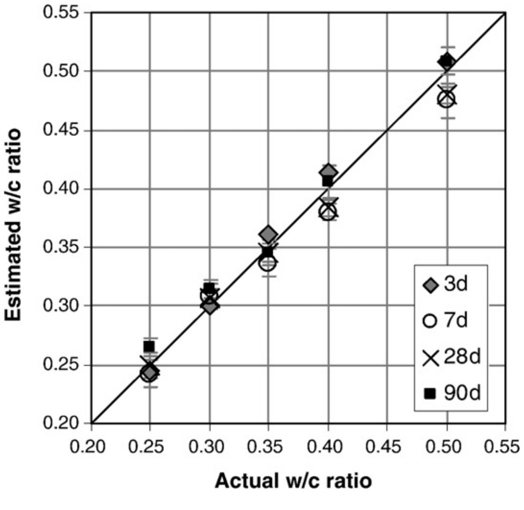

**Fig. 5.** Comparison between the estimated and actual values of the water–cement ratio for all samples investigated. The error bars represent 95% confidence interval.

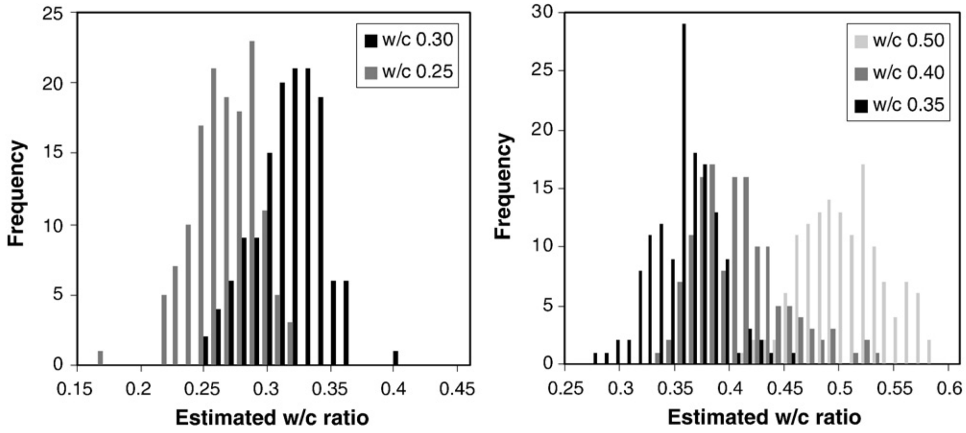

**Fig. 6.** Frequency distribution histograms indicating a significant spatial variation in the 'local' *w*/*c* ratio. Each histogram plot is obtained from 120 data points (30 frames per sample per curing age).

due to the decomposition of other volatile phases, such as carbonates, which would make the LOI results higher than actual values.

The errors in estimating the original cement content, water content and the free *w*/*c* ratio ranged from −30 to +50 kg/m$^3$ (−1.7 to +3.7%), −9 to +18 kg/m$^3$ (−1.6 to +4.1%) and −0.025 to +0.015 (−5 to +6%) respectively. For degree of hydration, the percentage estimation errors ranged from −11.3 to +7.2% and −2.0 to +2.7% when comparing to the LOI method and conventional image analysis method respectively. It is interesting to note that the agreement of within ±10% from the LOI method is similar to the results obtained by Feng et al. [23], who used an SEM point-counting technique for estimating hydration degree. The magnitude of error for all estimations does not appear to be influenced by either *w*/*c* ratio or curing age.

As expected, the proposed method is sensitive to $\delta_V$. For example, by using a $\delta_V$ value of 2.2 instead of 2.02 (i.e. ~9% increase in $\delta_V$), the range of percentage estimation error for *w*/*c* ratio increases to +5 to +14.3%. Therefore, the $\delta_V$ value must be accurately determined for a particular cement composition and the experimental results from Powers and Brownyard [14] can be used for this purpose (section 2.2). We have analysed about 170 values taken from Powers and Brownyard [14] (Tables 2–7, p. 596–601 of ref. 14) for pastes and mortars prepared from the 86 cement types representing a wide variation in composition ($C_3S$: 23–63%; $C_2S$: 9.3–56%; $C_3A$: 1.2–15%; $C_4AF$: 5.5–22%, from Table A2, p.305–307 of ref. 14), *w*/*c* ratio (0.31–0.61) and curing age (7–479 days). Considering such a wide range of samples, the calculated $\delta_V$ from the original data varied only between 1.8 and 2.3, with mean and median values of 2.13 and 2.15 respectively. However, many cements tested by Powers and Brownyard [14] have a relatively low $C_3S$ content, unlike contemporary Portland cements. Nevertheless, Powers and Brownyard [14] also tested cements with high $C_3S$ contents, for example cements 13753, 14560, 15498, 15758, 15924 and 15925 (with $C_3S$: 60–63%; $C_2S$: 12–17%; $C_3A$: 4–11%, $C_4AF$: 8–14%) and samples made with these have a calculated $\delta_V$ of 2.0–2.1, which is close to the value used in this study.

## 5. Discussion

The preliminary results show that the proposed method is applicable to ordinary Portland cement pastes with a range of *w*/*c* ratio (0.25 to 0.50) and curing ages (3 to 90 days) and we expect that the method to be extendable to Portland cement mortars and concretes as well. The presence of aggregates does not influence the model because their volume fraction is constant with time therefore Eq. (1) holds. However, aggregates will increase the paste heterogeneity due to wall-effect and micro-bleeding causing the interfacial transition zone phenomena, hence more images may need to be captured and analysed to obtain representative results.

The advantage of the proposed method is that it is able to make separate estimations of the original cement and water content, which is then used to determine the original *w*/*c* ratio. This can be carried

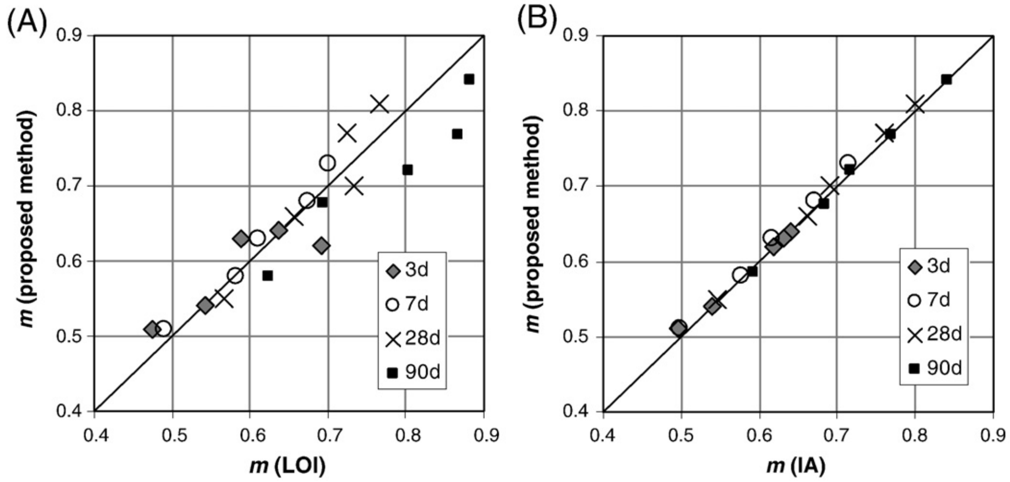

**Fig. 7.** Comparison between the estimated degree of hydration using the proposed method (Eq. (5)) and the measured degree of hydration from (A) loss-on-ignition and, (B) conventional image analysis method (Eq. (10)).

out without referring to calibration or reference standards, or having prior knowledge of the mix proportions. The method also does not appear to be influenced by hydration degree and curing age. Another advantage of the proposed method is that it can determine the hydration degree of samples with unknown cement content and samples with aggregates, such as mortars and concretes. Measurement of hydration degree of mortars and concretes using the LOI technique is difficult because the aggregates must first be separated from the paste, so that the original cement content can be obtained from the mass remaining at the end of ignition. The aggregates can be isolated by either crushing followed by sieving, or by dissolving the paste with concentrated acid, but both methods are known to be not very effective. As such, the hydration degree of mortars and concretes are often determined from LOI of parallel cement pastes that have undergone the same curing regime, but the accuracy of this is also questionable.

In Eq. (1), we have assumed that the total shrinkage is small and negligible for the purpose of *w*/*c* ratio estimation. If drying shrinkage is considered, then the formula for *w*/*c* ratio, derived following the same principle can be written as:

$$\frac{w}{c} = \frac{(V_{HP} + V_S)(\delta_V - 1) + \delta_V V_{CP}}{(\delta_V V_{AH} + V_{HP} + V_S)\rho_c} \qquad (11)$$

where $V_s$ is the change in volume of the hydration products due to loss of adsorbed water, which in theory, can be approximated as the loss of a water layer of one molecule thick from the surface of all gel particles [1]. Since the thickness of a water molecule is about 1% of the gel particle size, upon complete drying, a linear change in dimension from shrinkage ($\varepsilon_s$) is expected to be of the order of $10^4$ microstrain. In practice, values of up to $4\times10^3$ microstrain have been observed in pastes [1]. Taking the upper bound value of $\varepsilon_s = 10^4$ microstrain, the total amount of shrinkage ($V_s$) is only 0.1%, which translates to a difference in the estimated *w*/*c* ratio (from Eqs. (4) and (11)) of no more than 0.0005 for all the samples investigated.

As in the case of the other techniques currently available for estimating *w*/*c* ratio, the proposed method can only be applied to samples that are sound and in no way damaged, either physically or chemically. The samples must not have experienced substantial volumetric change, either excessive shrinkage or expansive reaction such that Eq. (1) no longer applies, and reactions that may affect the porosity (e.g. carbonation and leaching) or change the characteristics of the hydration products formed. However, the proposed method may be applicable to concretes that are poorly compacted and with entrained air by carefully excluding the volume fractions of air voids during image analysis. The method is also not affected by bleeding or absorption into porous aggregates as it calculates the free *w*/*c* ratio. Samples with excessive bleeding will show a larger spread in the local *w*/*c* ratio, therefore requiring more images to be averaged to obtain accurate results.

The image resolution used in this study may not be sufficient to characterise the entire range of capillary pores, in particular those finer than the pixel spacing (~0.1 µm). At present, pores finer than the pixel spacing are considered as part of the hydration products. As mentioned earlier, this pixel spacing was chosen as a compromise between achieving adequate sampling size and resolution. The sample can be analysed at a higher magnification and resolution, but because of the smaller field of view, this will come at a cost of increased effort and time since substantially more images must be processed for statistical significance. In addition, image segmentation is never a perfect, error free procedure. Nevertheless, the image digitisation and segmentation can be viewed as an averaging process and small errors from segmentation and finite resolution may actually not have a significant effect on the final result. However, the accuracy of the method when used on data derived from a conventional tungsten filament SEM is unknown. Additional work is needed to study the effect of image magnification and resolution on the accuracy of the proposed method.

In practice, samples with high *w*/*c* ratio (>0.5) will be of most interest in the context of resolving disputes due to suspected non-compliance with the mix specification. Unfortunately, the current study is limited to an upper *w*/*c* ratio of 0.5. This was because of difficulties in avoiding segregation during preparation of paste samples that have very high *w*/*c* ratio. However, our future study will include mortars and concretes samples with *w*/*c* ratio greater than 0.5. Samples with high *w*/*c* ratio will have a greater fraction of larger capillary pores, and therefore this reduces the error caused by finite resolution of the imaging system.

Supplementary cementitious materials are increasingly being utilised in modern concretes. At present, we have not included supplementary cementitious materials in the model, so this will be another major focus of our future work. Clearly, application of the method to samples with binders other than Portland cement will require special considerations. The overall principle of the method appears to be sound as long as an appropriate $\delta_V$ is specified according to the cement type, but certain assumptions, for instance the constancy of $\delta_V$ with *w*/*c* ratio, curing age and exposure needs to be re-examined for these materials. The accuracy of $\delta_V$ derived from Powers and Brownyard's model warrants further examination, and this approach may be refined in future studies. Clearly more work is needed to assess how robust the proposed method is when applied to a larger range of cement-based materials, including field samples and various processing and curing methods.

## 6. Conclusion

In this paper, we proposed a new microscopy-based method for estimating the cement content, water content and free *w*/*c* ratio of Portland cement-based materials with unknown mixture proportions and degree of hydration. The method first measures the volume fractions of the unreacted cement, hydration products and capillary pores using field emission scanning electron microscopy in the backscatter mode, then calculates the original cement content, free water content and free *w*/*c* ratio. The same method can also be used to calculate the degree of hydration. The proposed method makes use of the volumetric ratio of hydration products to the reacted cement ($\delta_V$), which is known from previous studies to be slightly dependent on the cement composition, but invariant to *w*/*c* ratio and curing age. This method has the advantage that it is quantitative, and does not require comparison with reference samples made with the same materials and cured to the same hydration degree as the tested sample. Preliminary results are encouraging, whereby a good agreement was observed between the estimated and actual values for ordinary Portland cement pastes with a range of *w*/*c* ratios (0.25–0.50) and curing ages (3–90 days). The error in determination for the *w*/*c* ratio was no more than 0.025. Future studies will aim to extend the application of the proposed method to blended cements, mortars and concretes.

## Acknowledgements

HSW acknowledges the support provided by the EPSRC Platform Grant for the Concrete Durability Group (EPSRC GR/M97206). We thank the reviewers for their constructive comments and suggestions.

## References

[1] A.M. Neville, Properties of Concrete, Fourth EditionAddison Wesley Longman Ltd., 1995.

[2] A.M. Neville, How closely can we determine the water–cement ratio of hardened concrete, Mat. Struct. 36 (2003) 311–318.

[3] BS 1881: Part 124: 1988, Methods for Analysis of Hardened Concrete, British Standards Institution.

[4] Concrete Society, Analysis of hardened concrete, Tech. Rep. 32 (1989) 110.

[5] D.A. St. John, A.W. Poole, I. Sims, Concrete Petrography, Arnold and John Wiley & Sons, London, 1998 474 pp.

[6] NT Build 361-1999, Concrete, Hardened: Water–Cement Ratio, Nordtest Method, Edition 2, 1999.

[7] P. Christensen, H. Gudmundsson, H. Thaulow, A.D. Damgard-Jensen, S. Chatterji, Structural and ingredient analysis of concrete — methods, results and experience, Nord. Betong 3 (1979) 4–9.

[8] B. Mayfield, The quantitative evaluation of the water/cement ratio using fluorescence microscopy, Mag. Concr. Res. 42 (150) (1990) 45–49.

[9] J. Elsen, N. Lens, T. Aarre, D. Quenard, V. Smolej, Determination of the w/c ratio of hardened cement paste and concrete samples on thin sections using automated image analysis techniques, Cem. Concr. Res. 25 (4) (1995) 827–834.

[10] U.H. Jakobsen, P. Laugesen, N. Thaulow, Determination of water–cement ratio in hardened concrete by optical fluorescence microscopy, water–cement ratio and other for determination, in: M.S. Khan (Ed.), SP 191-3, ACI International, Los Angeles, 1998, pp. 27–41.

[11] S. Sahu, S. Badger, N. Thaulow, R.J. Lee, Determination of water–cement ratio of hardened concrete by scanning electron microscopy, Cem. Concr. Compos. 26 (8) (2004) 987–992.

[12] H.F.W. Taylor, Cement Chemistry, Second editionThomas Telford, London, 1997 459 pp.

[13] D.P. Bentz, Three-dimensional computer simulation of Portland cement hydration and microstructure development, J. Am. Ceram. Soc. 80 (1) (1997) 3–21.

[14] Powers, T.C., Brownyard, T.L. (1946–1947), Studies of the physical properties of hardened Portland cement paste, Bull. 22, Res. Lab. of Portland Cement Association, Skokie, IL, USA, reprinted from J. Am. Concr. Inst. (Proc.) Vol 43 in 9 parts, pp. 101–132, 249–336, 469–504, 549–602, 669–712, 845–880, 933–992.

[15] T.C. Hansen, Physical structure of hardened cement paste. A classical approach, Mat. Struct. 19 (1986) 423–436.

[16] H.J.H. Brouwers, The work of Powers and Brownyard revisited: part 1, Cem. Concr. Res. 34 (2004) 1697–1716.

[17] K.L. Scrivener, Backscattered electron imaging of cementitious microstructures: understanding and quantification, Cem. Concr. Compos. 26 (8) (2004) 935–945.

[18] J. Goldstein, D. Newbury, D. Joy, C. Lyman, P. Echlin, E. Lifshin, L. Sawyer, J. Michael, Scanning Electron Microscopy and X-Ray Microanalysis, Third EditionKluwer Academic/Plenum Publishers, New York, 2003 689 pp.

[19] H.F.W. Taylor, Modification of the Bogue Calculation, Adv. Cem. Res 2 (6) (1989) 73–77.

[20] H.S. Wong, N.R. Buenfeld, Patch microstructure in cement-based materials: fact or artefact? Cem. Concr. Res. 36 (5) (2006) 990–997.

[21] Underwood, E.E. (1970), Quantitative Stereology, Addision-Wesley, Reading, Massachusetts, 274p.

[22] H.S. Wong, M.K. Head, N.R. Buenfeld, Pore segmentation of cement-based materials from backscattered electron images, Cem. Concr. Res. 36 (6) (2006) 1083–1090.

[23] X. Feng, E.J. Garboczi, D.P. Bentz, P.E. Stutzman, T.O. Mason, Estimation of the degree of hydration of blended cement pastes by a scanning electron microscope point-count procedure, Cem. Concr. Res. 34 (10) (2004) 1787–1793.